Vitamin B6 biosynthesis by the malaria parasite Plasmodium falciparum: biochemical and structural insights

Gengenbacher, Martin; Fitzpatrick, Thérésa Bridget; Raschle, Thomas; Flicker, Karlheinz; Sinning, Irmgard; Müller, Sylke; Macheroux, Peter; Tews, Ivo; Kappes, Barbara

How to cite

GENGENBACHER, Martin et al. Vitamin B6 biosynthesis by the malaria parasite Plasmodium falciparum: biochemical and structural insights. In: The Journal of biological chemistry, 2006, vol. 281, n° 6, p. 3633–3641. doi: 10.1074/jbc.M508696200

This publication URL: https://archive-ouverte.unige.ch/unige:89536
Publication DOI: 10.1074/jbc.M508696200

Enzyme Catalysis and Regulation:

Vitamin B6 Biosynthesis by the Malaria Parasite *Plasmodium falciparum*: BIOCHEMICAL AND STRUCTURAL INSIGHTS

Martin Gengenbacher, Teresa B. Fitzpatrick, Thomas Raschle, Karlheinz Flicker, Irmgard Sinning, Sylke Müller, Peter Macheroux, Ivo Tews and Barbara Kappes

J. Biol. Chem. 2006, 281:3633-3641.
doi: 10.1074/jbc.M508696200 originally published online December 8, 2005

THE JOURNAL OF BIOLOGICAL CHEMISTRY VOL. 281, NO. 6, pp. 3633–3641, February 10, 2006

Vitamin B6 Biosynthesis by the Malaria Parasite *Plasmodium falciparum*

BIOCHEMICAL AND STRUCTURAL INSIGHTS[*] [S]

Received for publication, August 8, 2005, and in revised form, November 17, 2005 Published, JBC Papers in Press, December 8, 2005, DOI 10.1074/jbc.M508696200

Martin Gengenbacher[‡], Teresa B. Fitzpatrick[§], Thomas Raschle[§1], Karlheinz Flicker[¶], Irmgard Sinning[‖], Sylke Müller[2], Peter Macheroux[¶3], Ivo Tews[‖4], and Barbara Kappes[‡5]**

*From the [‡]Abteilung für Parasitologie, Universitätsklinikum Heidelberg, Im Neuenheimer Feld 324, D-69120 Heidelberg, Germany, the [§]Eidgenössische Technische Hochschule Zürich, Institut für Pflanzenwissenschaften, Universitätsstrasse 2, CH-8092 Zürich, Switzerland, the [¶]Technische Universität Graz, Institut für Biochemie, Petersgasse 12, A-8010 Graz, Austria, the [‖]Department of Structural Biology, Biochemiezentrum der Universität Heidelberg, Im Neuenheimer Feld 328, D-69120 Heidelberg, Germany, and the **Institute of Biomedical and Life Sciences, Division of Infection and Immunity, University of Glasgow, Glasgow G12 8QQ, Scotland, United Kingdom*

Vitamin B6 is one of nature's most versatile cofactors. Most organisms synthesize vitamin B6 via a recently discovered pathway employing the proteins Pdx1 and Pdx2. Here we present an in-depth characterization of the respective orthologs from the malaria parasite, *Plasmodium falciparum*. Expression profiling of Pdx1 and -2 shows that blood-stage parasites indeed possess a functional vitamin B6 *de novo* biosynthesis. Recombinant Pdx1 and Pdx2 form a complex that functions as a glutamine amidotransferase with Pdx2 as the glutaminase and Pdx1 as pyridoxal-5′-phosphate synthase domain. Complex formation is required for catalytic activity of either domain. Pdx1 forms a chimeric bi-enzyme with the bacterial YaaE, a Pdx2 ortholog, both *in vivo* and *in vitro*, although this chimera does not attain full catalytic activity, emphasizing that species-specific structural features govern the interaction between the protein partners of the PLP synthase complexes in different organisms. To gain insight into the activation mechanism of the parasite bi-enzyme complex, the three-dimensional structure of Pdx2 was determined at 1.62 Å. The obstruction of the oxyanion hole indicates that Pdx2 is in a resting state and that activation occurs upon Pdx1-Pdx2 complex formation.

Plasmodium falciparum is the causative agent of severe malaria. Each year up to two million human deaths and enormous economic losses are attributed to this parasite. Drug resistance in *P. falciparum* has been aggravating the problem in many parts of the world during the last two decades, which considering the lack of a protective vaccine, is the major obstacle to combat the disease. Hence, new antimalarials are urgently needed. Requirements for nutrients and vitamins have previously been discussed as possible novel targets (1). Indeed the *P. falciparum* genome contains genes that encode enzymes necessary for the syntheses of the vitamin precursor chorismate (2–4), vitamin B6 (5, 6), and the vitamin-like cofactor lipoic acid (7).

Vitamin B6 is renowned in the medical field as being involved in more bodily functions than any other single nutrient. It is required for the maintenance of physical as well as mental health. The term "vitamin B6" collectively refers to the vitamers pyridoxal, pyridoxine, and pyridoxamine, and their respective phosphate esters. The metabolically active form is pyridoxal 5′-phosphate (PLP),[6] an essential co-enzyme in numerous pathways such as amino acid metabolism and the biosynthesis of antibiotic compounds. In contrast to mammals, which have to take up vitamin B6 from their diet, bacteria, fungi, plants, and the protozoan *P. falciparum* have the ability to synthesize the vitamin *de novo*.

Analyses of a number of available genomes has demonstrated that most organisms, including all archaea, fungi, plants, and protozoa and most eubacteria use a class I glutamine amidotransferase (GATase) composed of two domains, a glutaminase and its associated acceptor/synthase domain to generate vitamin B6 (8–13). Structural knowledge on class I GATases in general demonstrates a common fold for the glutaminase subunit, whereas structure and function of the interacting synthase subunits vary (14). The synthase subunit appears to have a protein tunnel, which connects the glutaminase and synthase active sites and shields the labile ammonia produced by the glutaminase. The glutaminase is dependent on the interaction with the synthase, and both active sites are structurally and biochemically linked (14, 15).

The GATase involved in vitamin B6 biosynthesis is a bi-enzyme complex consisting of Pdx1, the acceptor/synthase, and Pdx2, the glutaminase domain (16, 17). Very recently, the substrates of Pdx1 and the biosynthetic pathway have been described for the *Bacillus subtilis* orthologs YaaD and YaaE. In contrast to *Escherichia coli*, which possesses an alternative enzymatic machinery for vitamin B6 biosynthesis (11), this pathway directly results in PLP formation (18, 19).

In the malaria parasite *P. falciparum*, single genes encoding Pdx1 and

* This work was supported in part by the European Commission (Grant VITBIOMAL-012158). Data collection was performed at beamline ID29 (ESRF, Grenoble). The costs of publication of this article were defrayed in part by the payment of page charges. This article must therefore be hereby marked "*advertisement*" in accordance with 18 U.S.C. Section 1734 solely to indicate this fact.

The nucleotide sequence(s) reported in this paper has been submitted to the GenBank™/EBI Data Bank with accession number(s) DQ077732.

The atomic coordinates and structure factors (code 2ABW) have been deposited in the Protein Data Bank, Research Collaboratory for Structural Bioinformatics, Rutgers University, New Brunswick, NJ (http://www.rcsb.org/).

[S] The on-line version of this article (available at http://www.jbc.org) contains supplemental Figs. S1–S3.

[1] Supported by the Swiss National Science Foundation (Grant 3100A0-107975).

[2] A Wellcome Trust Senior Fellow.

[3] Thanks the Austrian Fonds zur Förderung der wissenschaftlichen Forschung for generous financial support (Grant FWF 17215).

[4] To whom correspondence may be addressed. Tel.: 49-6221-544788; Fax: 49-6221-544790; E-mail: ivo.tews@bzh.uni-heidelberg.de.

[5] To whom correspondence may be addressed. Tel.: 49-6221-561774; Fax: 49-6221-564643; E-mail: barbara.kappes@urz.uni-heidelberg.de.

[6] The abbreviations used are: PLP, pyridoxal 5′-phosphate; APAD, 3-acetylpyridine adenine dinucleotide; CPS, carbamoyl phosphate synthase; DHAP, dihydroxyacetone phosphate; GATase, glutamine amidotransferase; G3P, glyceraldehyde 3-phosphate; ImGPS, imidazole glycerol phosphate synthase; RBS, ribosomal binding site; MES, 2-(*N*-morpholino)ethanesulfonic acid; IPTG, isopropyl 1-thio-β-D-galactopyranoside; r.m.s.d., root mean square deviation; TMM, Spizizens minimal medium supplemented with 0.5 mM L-tryptophan and 10 mg ml^{-1} $FeSO_4 \times 7H_2O$.

Pdx2 have been identified (5, 6). This study reports a detailed biochemical and cellular analysis of the Pdx1-Pdx2 bi-enzyme complex. Furthermore, we report the three-dimensional-structure of Pdx2 and compare it with those of known class I GATases. In view of the absence of vitamin B6 biosynthesis in the mammalian host, this study is aimed to obtain further insights into the suitability of this metabolic pathway for the design of new antimalarials.

MATERIALS AND METHODS

Parasites—*P. falciparum* isolate K1 (Thailand), adapted to growth in horse serum, was a gift of Dr. Matile (F. Hoffmann-La Roche, Basel). *P. falciparum* HB3 and 3D7 were provided by Prof. Lanzer (University of Heidelberg, Germany). *P. falciparum* K1 was cultured as described (20). *P. falciparum* HB3 and 3D7 were cultivated according to Trager and Jensen in RPMI 1640 medium containing 5% human serum A^+ under reduced oxygen (21). The techniques of parasite synchronization, isolation, lysis, and protein preparation as well as the separation of the cellular fractions were performed as described previously (22). The concentration of acivicin required to inhibit parasite growth by 50% after 48 h (IC_{50}) was determined by the method of [G-^{3}H]hypoxanthine incorporation (23), using cultures of 1% hematocrit and 0.8% initial parasitemia.

Data Base Searches and Sequence Analyses—Genes apparently encoding Pdx1 and Pdx2 were identified in the *Plasmodium* genome data base PlasmoDB (PlasmoDB.org (24)) by performing TBLASTN searches using the protein sequences from *B. subtilis* (accession numbers: P37527 for YaaD, *B. subtilis* Pdx1 ortholog; P37528 for YaaE, *B. subtilis* Pdx2 ortholog).

Molecular Biological Methods—The full-length *Pdx1* and *Pdx2* genes and/or cDNAs of *P. falciparum* were amplified by PCR using sequence-specific sense and antisense oligonucleotides and *P. falciparum* 3D7 genomic or cDNA as template. To express the predicted full-length proteins, the PCR fragments were cloned into the NdeI and XhoI sites of pET-21a(+) (Novagen). Cloning into the NdeI site allows the use of the native methionine for expression. Two extra amino acids plus a His_6 tag are added to the C terminus by using the XhoI site. The *Plasmodium berghei Pdx2* cDNA was amplified from cDNA of the *P. berghei* NK56 strain by PCR using sequence-specific sense and antisense oligonucleotides derived from the *PbPdx2* gene of the *P. berghei* ANKA strain. The nucleotide sequences of all constructs were confirmed by automated sequencing.

Recombinant Expression, Purification, and Enzyme Assays—Pdx1 and -2 were expressed in the *E. coli* strain BL21-CodonPlus®(DE3)-RIL (Stratagene) using standard protocols. After 3 h (Pdx1) or 5 h (Pdx2) bacteria were harvested by centrifugation, resuspended in lysis buffer (300 mM NaCl, 10 mM imidazole, 5 mM β-mercaptoethanol, 50 mM Tris-HCl, pH 8.0, containing 1 mM phenylmethylsulfonyl fluoride, 2 mM benzamidine), flash-frozen, and stored at −80 °C.

Cells were disrupted by sonication, and the suspension was cleared by centrifugation. The crude supernatant was applied to nickel-nitrilotriacetic acid (Qiagen), washed with 600 mM NaCl, 5 mM β-mercaptoethanol, 50 mM Tris-HCl, pH 8.0, containing either 10 (Pdx2) or 40 mM imidazole (Pdx1) and eluted with 300 mM NaCl, 200 mM imidazole, 5 mM β-mercaptoethanol, 50 mM Tris-HCl, pH 8.0. For storage, glycerol was added to a final concentration of 10%, and the protein was frozen at −80 °C.

Pdx2 was further purified on a Superdex™ 200 26/60 gel filtration column (Amersham Biosciences) equilibrated with 20 mM Tris-HCl, pH 8.0, containing 200 mM NaCl and 1 mM dithiothreitol. Pdx2 eluted at a volume of 240 ml corresponding to an apparent molecular mass of 25 kDa consistent with Pdx2 being a monomer in solution. For crystallization, fractions containing monomeric Pdx2 were concentrated to >30 mg/ml.

To investigate complex formation of Pdx1 and -2, the respective genes were cloned into pETDuet™-1 (Novagen). A stop codon and a PacI site were introduced at the 3′-end of *Pdx1*. In the case of *Pdx2*, a NcoI site was introduced at the 5′-end and a His_6 tag, a stop codon, and a NotI site at the 3′-end. *Pdx1* was cloned into the multiple cloning site 2 via NdeI/PacI and *Pdx2* into multiple cloning site 1 via NcoI/NotI. The nucleotide sequence of the construct was confirmed by automated sequencing. Expression and purification of the complex were performed as described for Pdx2.

Different molar ratios of Pdx1 and -2 were analyzed for glutaminase activity using a coupled enzymatic assay with glutamate dehydrogenase as described (17). The reduction of NAD^+ to NADH was monitored at 340 nm (ϵ_{NAD} = 6220 M^{-1} cm^{-1}). Samples were prepared in a total volume of 300 μl containing 50 mM Tris-HCl, pH 8.0, 2 mM L-glutamine (Sigma-Aldrich), 9 μM Pdx2, and Pdx1 at varying concentrations covering a molar equivalent range of 0 to 2 (moles of Pdx1/moles of Pdx2). For kinetic analyses, glutaminase activity of Pdx2 was determined online using a modification of the above described method. For each measurement Pdx1 and -2 at equimolar concentrations were added to quartz cuvettes containing a freshly prepared mixture of 0.5 mM 3-acetylpyridine adenine dinucleotide (APAD), an analog of NAD^+, 30 units of bovine glutamate dehydrogenase, and buffer (50 mM Tris-HCl, pH 8.0, 1 mM EDTA). The reaction was started by adding 0–30 mM L-glutamine to a final volume of 600 μl. Reduction of APAD to APADH was measured at 363 nm (ϵ_{APADH} = 8900 M^{-1} cm^{-1}) at 30 °C.

The activity of Pdx1 was monitored according to a previous study (19). Reactions were carried out in 50 mM Tris-HCl, pH 8.0, at 37 °C containing 20 μM of the isolated Pdx1 and/or -2 and 1 mM of the substrates; either ribose 5-phosphate or ribulose 5-phosphate and either dihydroxyacetone phosphate or DL-glyceraldehyde 3-phosphate (2 mM). As a nitrogen source either 10 mM glutamine or 10 mM ammonium sulfate was added. In all cases samples were preincubated for 30 min in the presence of all components of the reaction apart from the triose sugar.

Acivicin inhibition was performed essentially as described before (19). The time course for the fraction of catalytic activity remaining displayed pseudo-first order kinetics from which the rate of inactivation (k) was determined by a fit of the data to the exponential function $f = e^{-kt}$. The second order rate constant was calculated from a plot of k *versus* the initial acivicin concentration.

Complementation Assay—pSWEET-*bgaB* was kindly provided by Amit P. Bhavsar, McMaster University, Hamilton, Ontario, Canada (25). To create pSWEET-expressing *Pdx1*, a PacI site and nucleotides −24 to −1 of the *B. subtilis tagD* gene providing a ribosomal binding site (RBS) were introduced at the 5′-end and a stop codon and a BamHI at the 3′-end of *Pdx1* and cloned into the PacI/BamHI sites of pSWEET. As a control, the same construct without the RBS was generated. Integration into the *B. subtilis* chromosome at the *amyE* locus via double recombination was selected with chloramphenicol (10 μg ml^{-1}) and confirmed by integration PCR.

The *B. subtilis* 168 (*trpC2*) *yaaD* disruptant was grown at 37 °C in TMM (Spizizen's minimal medium supplemented with 0.5 mM L-tryptophan and 10 mg ml^{-1} $FeSO_4 \times 7H_2O$) as described by Sakai and coworkers (26) in the presence of erythromycin (0.3 μg ml^{-1}) and 0.05 mM pyridoxal (27). IPTG (0.05 mM) was added for expression of down-

TABLE 1
Crystallographic data

A) Data collection statistics	
Spacegroup	C2
Cell a/b/c (Å); α, β, γ (°)	88.0/67.9/70.3; 90/92.3/90
Number of molecules per asymmetric unit	2
Resolution (Å)	25.0–1.62 (1.63–1.62)
R_{sym} (%)[a]	6.4 (46.6)
I/σI	19.3 (2.3)
Completeness (%)	99.9 (100.0)
Redundancy	5.2 (4.8)
Unique reflections	52,656
Average B (Å^2)	19.1
B) Refinement statistics	
R_{work} (%)[b]	15.3
R_{free} (%)[c]	18.9
Amino acids in model (range)	A2–A123, A128–A221, and B2–B227
Double conformations modeled	A2, A4, A9–A11, A27–A29, A55, A87, A100–A101, A111, A120, A134, A181, B39, B59, B87, B98, B104–B105, B109, B111, B121–B122, B130, B134, B136, B159–B160, B173, B179–180, B193, B219, and B221
No. of protein atoms	3648
No. of water atoms	469
No. of ligand atoms	13 (polyethylene glycol 200)
r.m.s.d. bond (Å)	0.023
r.m.s.d. angle (°)	1.962

[a] $R_{sym} = \Sigma_h\Sigma_i\ I(h) - I(h)_i\ /\Sigma_h\Sigma_i I(h)_i$, where $I(h)$ is the mean intensity after rejections.
[b] $R_{work} = \Sigma_h||F_{obs}(h) - F_{calc}(h)||/\Sigma h\ F_{obs}(h)$, where $F_{obs}(h)$ and $F_{calc}(h)$ are observed and calculated structure factors, respectively.
[c] 5% of the data were excluded to calculate R_{free}.

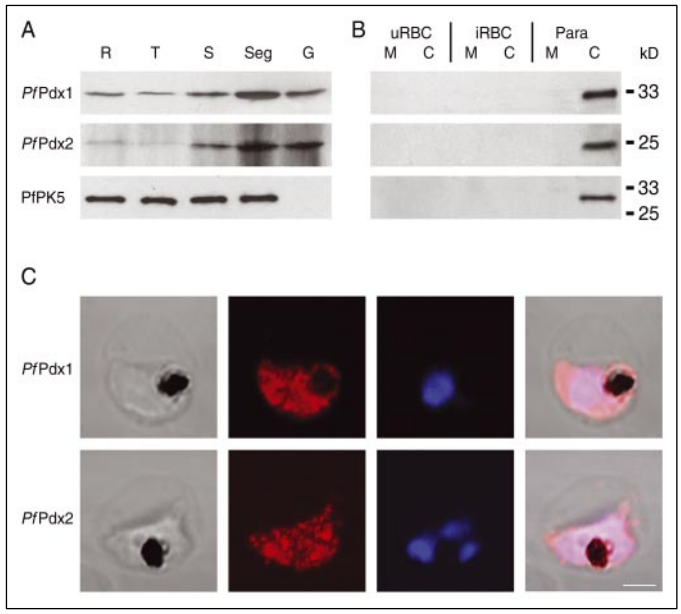

FIGURE 1. *A*, stage-specific immunoblot analysis of *P. falciparum* lysates. The blot was probed with antibodies against Pdx1, Pdx2, and PfPK5. Red blood cell stages: *R*, ring stage parasites (12 ± 2 h); *T*, trophozoites (25 ± 2 h); *S*, schizonts (34 ± 2 h); *Seg*, segmenters (44 ± 2 h); *G*, gametocytes, presexual stages. *B*, cellular fractions of *P. falciparum*-infected red blood cells: *uRBC*, uninfected red blood cell (control); *iRBC*, infected red blood cell; *Para*, parasite; *M*, membrane/organelle; and *C*, cytosol specify the respective cellular fraction. Either 15 μg of either the respective stage-specific lysate or cellular fraction was loaded. *C*, localization of Pdx1 and -2 within the parasite. Confocal immunofluorescence analysis of a trophozoite (Pdx1) and a schizont (Pdx2). Each *row* represents images from a single parasite: *First column*, transmitted light; *second column*, Pdx1 and -2 immunofluorescence, respectively; *third column*, parasite DNA; *fourth column*, overlay of the first three columns. The *scale bar* represents 2 μm.

stream genes (27). For complementation assays, the *B. subtilis* 168 *yaaD* disruptant plus RBS-*Pdx1* strain and the control strain, *B. subtilis* 168 *yaaD* disruptant plus *Pdx1* were grown under the above-mentioned conditions except that pyridoxal was omitted from the minimal medium. Expression of *Pdx1* was induced by supplementation with 2% xylose.

Immunological Methods—The recombinant Pdx1 and -2 proteins were used to raise polyclonal rabbit antisera by Sigma. For affinity purification, Pdx1 and -2 were purified as described above. The storage buffer was exchanged for coupling buffer (0.1 M NaCl, 0.05 M Na_2CO_3, and 0.05 M $NaHCO_3$, pH 8.3). Coupling to Epoxy-activated Sepharose^{TM} 6B (Amersham Biosciences) was carried out according to the manufacturer's instructions. Antibodies were bound to the matrix at 4 °C. The beads were washed with 1× phosphate-buffered saline (137 mM NaCl, 2.7 mM KCl, 1.5 mM KH_2PO_4, 8.1 mM Na_2HPO_4, pH 7.5), and antibodies were eluted in 100 mM glycine, pH 2.8, and neutralized by the addition of 3 M Tris-HCl, pH 8.8.

Western blots were performed according to Kyhse-Andersen (28). The membranes were incubated with either an anti-His antibody (mouse monoclonal, Novagen) at a 1:1,000 dilution, the affinity-purified Ab*Pdx*1 at a 1:30,000 dilution, the affinity-purified Ab*Pdx*2 at a 1:500 dilution, and the AbPfPK5 at a 1:10,000. The blots were developed using the ECL system (Amersham Biosciences).

Confocal immunofluorescence analyses were performed as described previously (2, 29). Parasites were labeled with affinity-purified Ab*Pdx*1 at a dilution of 1:2000 and the affinity-purified Ab*Pdx*2 at a dilution of 1:100. The secondary antibody, a donkey anti-rabbit-Cy3 conjugate (Jackson ImmunoResearch Laboratories) was applied at a dilution of 1:400. Parasite DNA was stained with Hoechst dye (benzimide H33342, Calbiochem) at a concentration of 2 μg ml^{-1} during the secondary antibody incubation period. Microscope slides were examined using a confocal laser scanning microscope (LSM 510, Zeiss).

Crystallization, Data Collection, Structure Determination, and Refinement—Purified Pdx2 was used for crystallization experiments using hanging drop vapor diffusion at 19 °C. Crystals grew overnight from 30% polyethylene glycol 200, 5% polyethylene glycol 3000 buffered with MES at pH 6.0. The dimensions of the crystals were ~100 × 40 × 40 μm. Crystals were flash-frozen and stored under liquid nitrogen. Data to 1.62 Å were collected at 100 K at the beamline ID29 at the European Synchrotron Radiation Facility (ESRF) in Grenoble, France. The crystals belong to the monoclinic space group C2 with unit cell dimensions of a = 88.0 Å, b = 67.9 Å, and c = 70.3 Å with a β-angle of 92.3°. For data collection statistics see Table 1A.

The structure was determined with molecular replacement using the program MOLREP (30) and the structure of YaaE as a search model (PDB entry 1R9G (31)). The asymmetric unit contains two protein chains. For initial model update and refinement, the auto-building options of ARP/wARP were used (molecular replacement mode (32)). ARP/wARP was able to trace and assign 421 out of 454 protein residues, among those the His_6 tag of chain B, and placed 421 water molecules in the model. Untraced residues were residues A1 to A2, A103 to A107, A122 to A129, A175 to A179, and A221 to A227 in chain A and B1 to B2, B145 to B147, and B227 in chain B. Refmac5 (33) refinement cycled with ARP-waterpicking was iterated in three cycles with model building in O (34). The final model contains residues 2 to 123 and 129 to 221 in chain A and 2 to 227 in chain B. Sixteen double conformations have been modeled for chain A and 21 for chain B. One polyethylene glycol molecule containing four ethylene glycol monomers has been observed bound to the protein. The seven Ramachandran outliers (disallowed and generously allowed) include the catalytic cysteines Cys^{87A} and Cys^{87B}. Statistics of the final refined model can be seen from Table 1B.

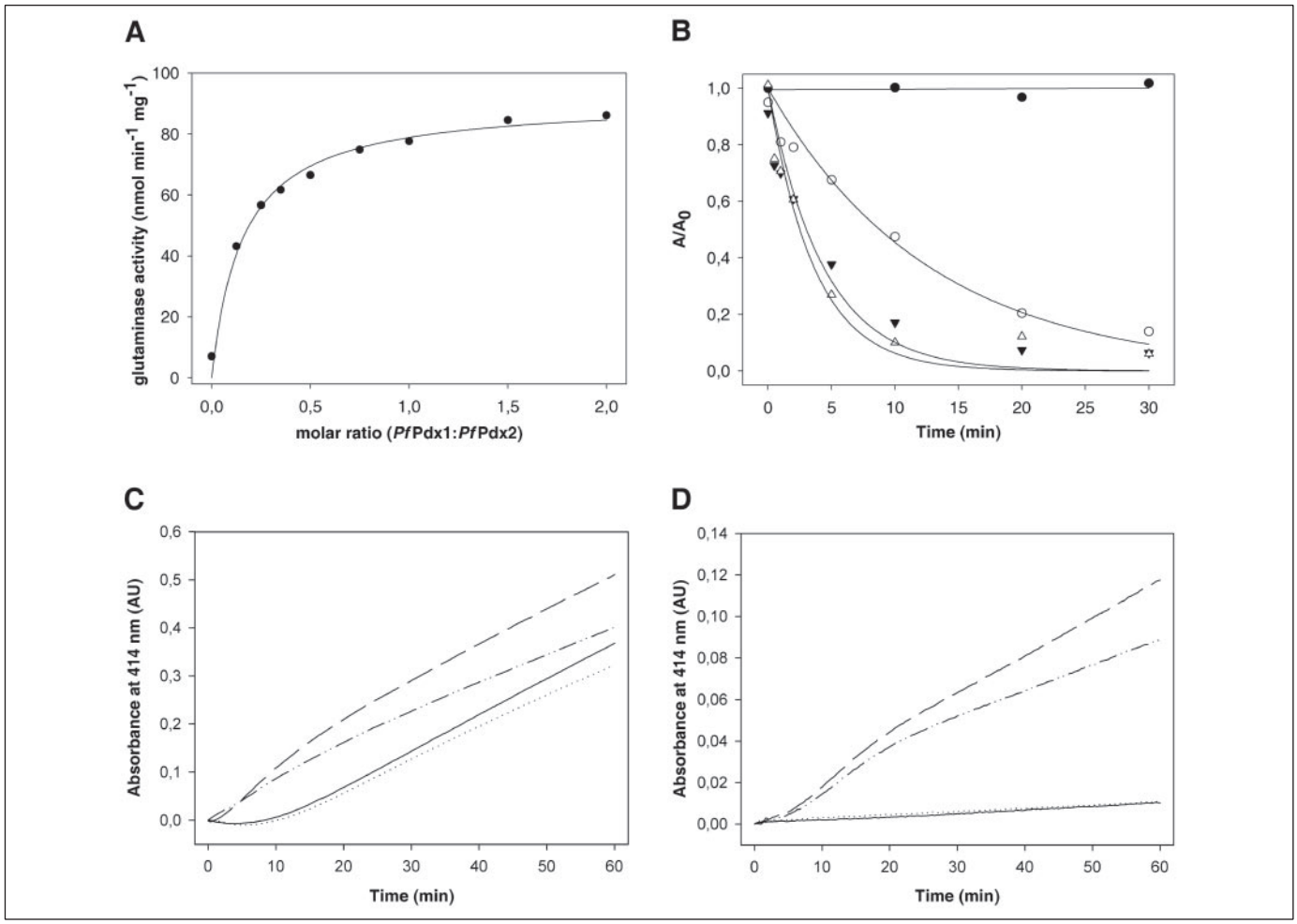

FIGURE 2. **Enzymatic characterization of Pdx1 and -2.** *A*, characterization of the glutaminase activity of Pdx2. Effect of Pdx1 on the glutaminase activity of Pdx2. *B*, effect of acivicin concentration on Pdx2 activity. The plot shows the fraction of glutaminase activity remaining (A/A_0) *versus* time in the presence of 0 mM (●), 5 mM (○), 10 mM (▼), and 15 mM (△) acivicin. The data were fitted to the exponential equation $f = e^{-kt}$. *C* and *D*, PLP synthase activity. *C*, PLP formation by the Pdx1-Pdx2 complex in the presence of glutamine (10 mM) or *D*, by Pdx1 in the presence of ammonium sulfate (10 mM): *dashed line*, ribose-5-phosphate and G3P; *solid line*, ribose-5-phosphate and DAHP; *dashed* and *dotted line*, ribulose 5-phosphate and G3P; and *dotted line*, ribulose 5-phosphate and DHAP. *Graphs* show representatives of five continuously recorded measurements.

RESULTS

Pdx1 and -2 Are Expressed in P. falciparum Blood Stages and Reside in the Parasite Cytosol—To assess that Pdx1 and Pdx2 are expressed during the erythrocytic life stages of *P. falciparum*, stage-specific parasite lysates were analyzed by Western blotting using antibodies generated against both recombinant proteins. Both proteins were detectable as single bands of the expected sizes (33 kDa for Pdx1 and 25 kDa for Pdx2) in all intraerythrocytic stages as well as in gametocytes (Fig. 1). It appears that the level of both proteins increases during the intraerythrocytic development with highest protein levels found in schizonts and segmenters. The blots were re-probed with an antibody of a protein expressed at equal levels throughout the erythrocytic cycle of the parasites (PfPK5, *P. falciparum* protein kinase 5) to control for equal loading (35).

A mixed stage parasite culture was fractionated into infected erythrocyte (*iRBC*) and parasite (*Para*), membrane/organelle (*M*), and cytosol (*C*) fraction to analyze the cellular distribution of Pdx1 and -2 in the parasites. Both proteins were exclusively detected in the parasite cytosol (Fig. 1*B*). An antibody against the control protein PfPK5 that is solely found in the parasite cytosol demonstrates the integrity of this fraction (35).

To visualize the cytosolic localization of Pdx1 and 2, intraerythrocytic parasites were analyzed by confocal immunofluorescence microscopy. Both Pdx1 and -2 show a disperse distribution within the parasite that is characterized by the absence of any discrete organelle specific pattern (Fig. 1*C*). Although many proteins show an even distribution within the cytosol, Pdx1 and -2 concentrate in part to diffuse foci. This has also been observed for example with the cytosolic *P. falciparum* chorismate synthase (2).

Pdx1 and -2 Are Required for Their Respective Enzyme Activities—Glutaminase activity of Pdx2 is only observed in the presence of Pdx1 as has also been observed by Wrenger *et al.* (7). A 1:1 molar ratio of the two proteins appeared to be optimal for glutaminase activity, indicative of a stoichiometric protein complex (Fig. 2*A*). Variation of the glutamine concentration produced typical Michaelis-Menten kinetics (data not shown) from which the kinetic constants were determined (k_{cat} as 0.11 s^{-1} and K_M as 0.56 mM).

Both ribose 5-phosphate and ribulose 5-phosphate, as well as glyceraldehyde 3-phosphate (G3P) and dihydroxyacetone phosphate (DHAP) are substrates for the plasmodial PLP synthase (Fig. 2*C*). The activity of the complex in the presence of G3P or DHAP was comparable when either ribose 5-phosphate (Fig. 2*C*, *dashed* and *solid lines*, respectively) or ribulose 5-phosphate (Fig. 2*C*, *dashed-dotted* and *dotted lines*, respectively) were used as the C5 sugars. Under the given assay conditions, the specific activity of the plasmodial PLP synthase was calculated to be 92.1 pmol min^{-1} mg^{-1} using ribose 5′-phosphate and G3P as substrates.

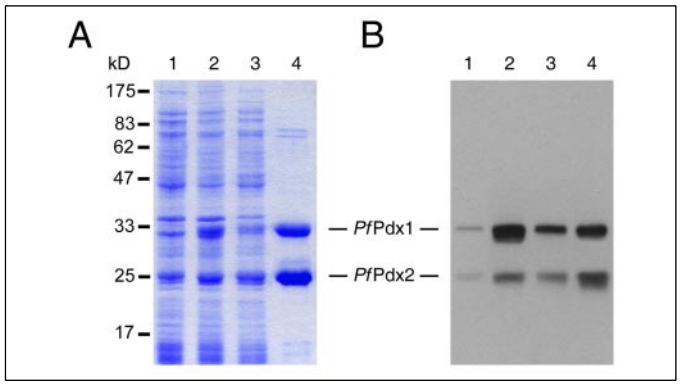

FIGURE 3. **Complex formation of Pdx1 and -2.** Co-expression of His-tagged Pdx2 and untagged Pdx1. *A*, Coomassie Brilliant Blue-stained SDS-PAGE gel (12%); *B*, Western blot analysis using the affinity-purified Ab*Pdx*1 and mouse monoclonal anti-His antibody for the detection of untagged Pdx1 and His-tagged Pdx2, respectively. *Lane 1*, uninduced cultures harboring the co-expression construct; *lane 2*, cultures induced with 0.4 mM IPTG; *lane 3*, lysate after sonication of cells and removal of cellular debris; *lane 4*, pooled fractions after affinity-purification by nickel-nitrilotriacetic acid chromatography.

When glutamine is used as the nitrogen donor (Fig. 2*C*), the activity of Pdx1 was found to be dependent on the presence of Pdx2 under all conditions. In the absence of Pdx2, however, ammonium sulfate can substitute for glutamine in the presence of either pentose sugar (Fig. 2*D*). However, ammonia could only be used by Pdx1 when G3P was used as the triose sugar (Fig. 2*D*: G3P plus ribose 5-phosphate (*dashed line*); G3P plus ribulose 5-phosphate (*dashed* and *dotted line*)). When DHAP was used, no reaction took place (Fig. 2*D*, *solid* and *dotted lines*), *i.e.* the reaction depended on complex formation with Pdx2.

In addition, it was shown that the two plasmodial proteins form a stable complex when co-expressed in the prokaryotic expression system used. The presence of both proteins during the expression and purification procedure was verified by Western blotting using the affinity-purified *Pdx*1 antibody and a monoclonal His tag antibody for the detection of Pdx2 (Fig. 3*B*). Both proteins were expressed at comparable levels, and affinity purification using nickel-nitrilotriacetic acid-agarose resulted in the co-purification of His-tagged Pdx2 and untagged Pdx1 (Fig. 3, *A* and *B*, *lane 4*).

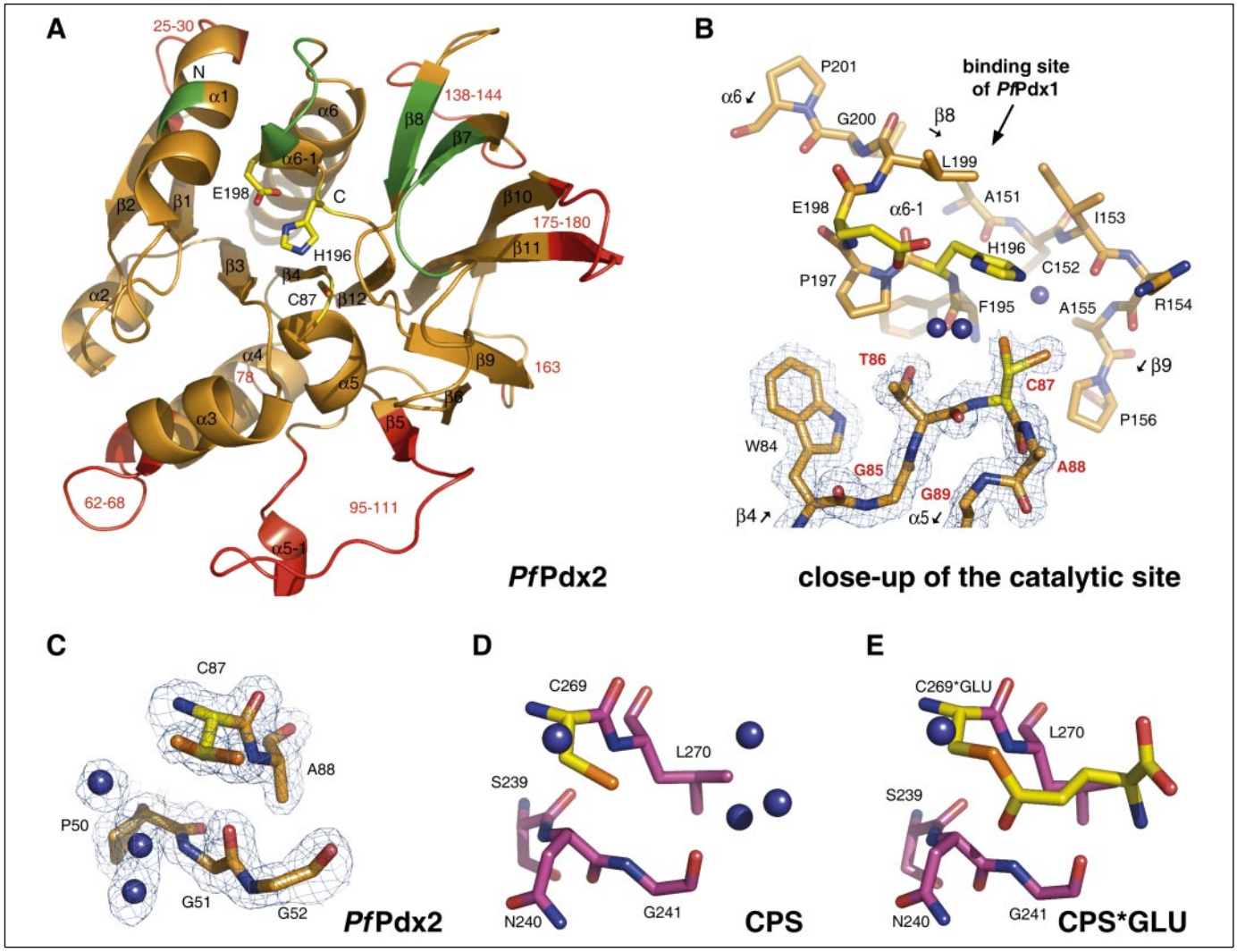

FIGURE 4. **Structural analysis of Pdx2.** *A*, *ribbon representation* of the x-ray structure of Pdx2. Amino acids Cys[87], His[196], and Glu[198] make up the catalytic triad. The respective residues are shown in *yellow* in all panels. Residues involved in the putative interface with the synthase subunit are labeled in *green*. Differences to the Yaa E ortholog are shown in *red*. *B*, *stick representation* of the active site of Pdx2. The loop carrying the nucleophilic cysteine comprises residues Gly[85], Thr[86], Cys[87], Ala[88], and Gly[89]. This loop is shown together with the $2F_o - F_c$ electron density at a level of 1.2σ. The double conformation of Cys[87] is visible. The proposed binding site of the synthase subunit is indicated. *C*, the proposed oxyanion hole, which forms during catalysis, is obstructed in Pdx2 by the carbonyl of Gly[51]. *D*, the oxyanion hole is formed in the apo-form of CPS (1JDB) by the peptide nitrogens of Gly[241] and Leu[270]. *E*, in the glutamine-bound state of CPS (1A9X), this conformation is maintained. The figure was prepared with PyMOL (53).

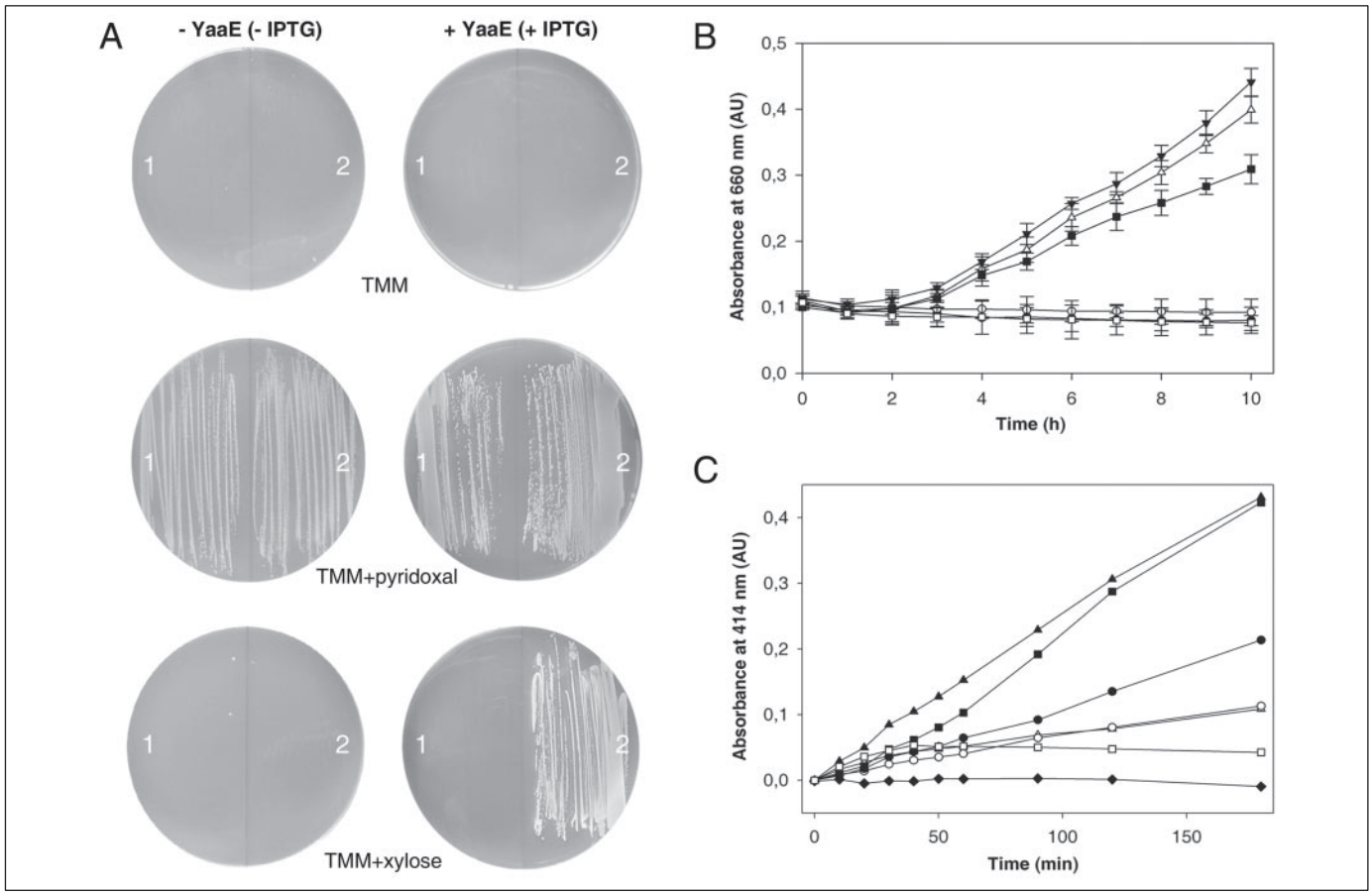

FIGURE 5. **Cross-species interaction between Pdx1 and YaaE.** *A*, growth of the *B. subtilis* 168 (*trpC2*) *YaaD* disruptant complemented with control construct lacking the ribosomal binding site (*Pdx1*) (*1*) or the complementation construct (RBS-*Pdx1*) (*2*) on minimal plates (*TMM*) without and with additives (0.05 mM pyridoxal (*TMM+pyridoxal*) or 2% xylose (*TMM+xylose*)) in the presence or absence of IPTG. IPTG is required to induce the expression of the endogenous *YaaE*. *B*, growth curves of the *B. subtilis* 168 (*trpC2*) *YaaD* disruptant complemented with RBS-*Pdx1* (*filled symbols*: ●, ▼, and ■) or the RBS-lacking *Pdx1* control construct (*open symbols*: ○, △, and □) in TMM plus IPTG without and with additives (0.05 mM pyridoxal or 2% xylose). ●, RBS-*Pdx1* in TMM; ○, *Pdx1* in TMM; ▼, RBS-*Pdx1* in TMM plus 0.05 mM pyridoxal; △, *Pdx1* in TMM plus 0.05 mM mM pyridoxal; ■, RBS-*Pdx1* in TMM − *Pdx1* expression was induced by the addition of 2% xylose; □, *Pdx1* in TMM plus 2% xylose. *C*, PLP formation by the Pdx1-YaaE complex in the presence of ribulose 5-phosphate, G3P, and 10 mM Gln: ▲, YaaD-YaaE complex (1:1); ■, Pdx1-Pdx2 complex (1:1); ●, Pdx1-YaaE (1:5); ○, Pdx1-YaaE (1:1); △, YaaD; □, Pdx1; ◆, no enzyme.

Effect of Acivicin on Pdx2 Activity and Parasite Growth—Acivicin irreversibly inhibits glutaminases by covalent modification of an essential cysteine residue (14, 36) and has been shown to inhibit the glutaminase subunit of PLP synthase from *B. subtilis* (19). Acivicin also inhibited Pdx2 in a concentration- and time-dependent manner (Fig. 2*B*). The loss in glutaminase activity appears as a pseudo-first order decay from which the rate constants for inactivation (k) could be calculated as $0.08 \pm 0.01\ min^{-1}$, $0.22 \pm 0.04\ min^{-1}$, and $0.27 \pm 0.04\ min^{-1}$, for 5 mM, 10 mM, and 15 mM acivicin, respectively. A plot of the pseudo-first order rate constants *versus* acivicin concentration was used to calculate the second order rate constant, $19 \pm 6\ min^{-1}\ M^{-1}$. In addition, the IC_{50} of acivicin on parasite growth was determined to be in the lower micromolar range (data not shown).

Structure Determination of Pdx2 and Comparison to That of Other GATases—To obtain insights into the precise architecture of the active site of Pdx2, the structure of the protein was determined by x-ray crystallography at 1.62 Å resolution. The mean coordinate error of the structure is 0.175 Å as derived from the Luzzati plot (30). The high resolution obtained is attributed at least in part to an interaction of two symmetry related molecules through a fully ordered hexa-histidine tag (see supplemental data).

The structure of Pdx2 is that of the classic mixed β-sheet of the glutaminase component of the triad GATases (Fig. 4*A*) (37). A large β-sheet in the center of the structure contains β-strands β2, β1, β3, β4, β12, β11, and β10, with all except β11 in parallel orientation. This central β-sheet is flanked by two small β-sheets. The first one is formed by the strands β5 and β6 in parallel orientation and β9 in an anti-parallel orientation. The second one contains the anti-parallel strands β7 and β8 and is instrumental in contacting the synthase subunit (see below (38)). Helices α1, α2, α3, α4, and α6 pack against the central β-sheet. The catalytic cysteine, Cys^{87}, lies in a sharp γ-like turn at the end of β-strand 4. The other two residues of the catalytic triad, His^{196} and Glu^{198}, are in a small helical segment in the loop region between the last β-strand, β12 and helix α6.

To identify differences of potential functional significance, the primary sequence and structure of Pdx2 were compared with other glutaminases: Pdx2 from *P. berghei* (*Pb*Pdx2; 63.8% amino acid identity), the bacterial ortholog YaaE from *B. subtilis* (37.1% amino acid identity (31)), and *Thermotoga maritima* HisH (16.5% amino acid identity; see supplemental data for alignment (39)). YaaE can be superimposed with Pdx2 with an r.m.s.d. of 1.47 Å (175 of 196 Cα positions from YaaE). Nonetheless, significant differences between the plasmodial and bacterial Pdx2s are observed. The most obvious one is an insertion between β5 and β6 in the malarial sequences not found in YaaE or in fact HisH (Fig. 4*A* and see alignment in supplemental data). In the Pdx2 structure these amino acids (95–111) form an additional, small helical segment, α5–1. Helix α4 of Pdx2 has an additional turn through an insertion at position 62–68. Both variable regions map to one side of the molecule

and result in a surface that is structurally different from YaaE. Another insertion in $Pdx2_{175-180}$ elongates the two β-strands β10 and β11 and points toward the potential interface with Pdx1 (see below). All other variations are located on the surface of the molecule opposite to the synthase interaction site, *e.g.* in loops $Pdx2_{25-30}$ and $Pdx2_{138-144}$.

Pdx2 is a typical triad glutaminase where the catalytic residues are Cys^{87}, His^{196}, and Glu^{198} (*yellow* in Fig. 4, *A* and *B*). The catalytic triad can be superimposed with an r.m.s.d. of 0.45 Å over all atoms with the respective YaaE residues Cys^{79}, His^{170}, and Glu^{172}. Other class I glutaminase active sites like HisH (IK9V) and carbamoyl phosphate synthase, CPS (1JDB (40)) superimpose similarly well. The loop that connects β4 and α5 harbors Cys^{87} in Pdx2 and is strictly conserved between Pdx2 and YaaE and highly conserved in glutaminases in general. The sequence Gly-Thr-Cys-Ala-Gly allows the catalytic residue in Pdx2 to adopt an unusual conformation in the disallowed region of the Ramachandran plot with phi/psi values of 54°–110° (Fig. 4*B*, amino acids are in *red lettering*). This constraint is essential for the catalytic function of triad GATases and has been described for the similar active sites of the structurally unrelated α/β hydrolase family of enzymes (41). In Pdx2 the side chain of Cys^{87} is observed in two conformations (Fig. 4, *B* and *C*). The ratio of these two rotamers was fitted to 0.55 and 0.45 in chain A and to 0.8 and 0.2 in chain B experimentally by setting the occupancy to obtain comparable *B*-values for the two rotamers after refinement. The rotamer with higher occupancy superimposed with the position of the catalytic cysteine of the His7 in the acivicin-bound state (1JVN (38)) and of CPS in the free and glutamine-bound states (1JDB, Fig. 4*D* (40) and 1A9X, Fig. 4*E* (42), respectively). The rotamer with lower occupancy pointing toward the catalytic histidine (Fig. 4*B*) is seen in a number of structures where the substrate binding pocket is occupied by ligands different from either substrate or product. Examples are GMP synthetase with a bound citrate (37), *Tm*ImGPS with a phosphate (1KXJ (43)) and *Tm*HisH with acetic acid in the substrate binding pocket (1K9V (39)).

A central feature of glutamine hydrolysis by triad GATases is the formation of an oxyanion hole during catalysis (44). In the glutaminase subunit of CPS the backbone nitrogens of Leu^{270} and Gly^{241} were suggested to participate in this structure (Fig. 4, *D* and *E*) (40, 42). The corresponding residues in Pdx2 (Ala^{88} and Gly^{51}) have a different main-chain conformation (Fig. 4*C*). The carbonyl oxygen of Gly^{51} points toward the potential oxyanion hole, suggesting that hydrolysis of glutamine cannot occur. Activation would then require the peptide bond of Gly^{51}/Gly^{52} to undergo peptide isomerization.

Because there is no structure of a PLP synthase complex present in the PDB data base (45), the putative interaction site between glutaminase and synthase subunits was analyzed based on the available GATase structures from different organisms. The closest structural relative to Pdx2 is HisH from *T. maritima*. Comparison with the imidazole glycerol phosphate synthase of *T. maritima* (HisH/HisF) and *Saccharomyces cerevisiae* (His7) allows to predict the contact sites for the interaction between the Pdx1 and -2 subunits of the plasmodial PLP synthase (38, 39). The glutaminase-synthase interaction surface involves many backbone contacts that are highly conserved in the three-dimensional structure (see regions labeled in *green* in Fig. 4*A*) but is not strictly conserved in primary structure. Pivotal in complex formation are β7 and β8 of the glutaminase. The interface of the complex also includes the loop region between β12 and α6 carrying the catalytic histidine and glutamate.

Pdx1 Can Substitute for YaaD Function in Vivo and in Vitro—The number of similarities between the PLP synthase of *B. subtilis* and *P. falciparum* and the high conservation of the predicted interaction surface of the glutaminase with the synthase subunit inspired us to perform functional complementation studies. A *B. subtilis* strain in which the *yaaD* gene, the Pdx1 ortholog, has been disrupted (*B. subtilis* 168 (*trpC2*) Δ*yaaD* (27)) was used for these investigations. Because this strain was generated using the vector pMutin 3, genes downstream of the target gene acquire an isopropyl-1-thio-D-galactoside-(IPTG)-inducible promoter to overcome polar effects transmitted from the disruption of the target gene (27, 46). Because *yaaE* is the downstream gene of *yaaD*, IPTG has to be added to the bacterial culture in minimal medium to induce expression of YaaE.

Two different constructs of *Pdx1* cloned into the expression vector pSWEET (25) were used for the complementation assays. One construct contains the coding sequence of Pdx1 with a ribosome binding site (RBS-*Pdx1*), whereas the other is lacking the ribosomal binding site (*Pdx1*) and thereby prohibiting translation of the parasite protein. Complementation was assessed both on minimal plates and in minimal liquid medium (Fig. 5, *A* and *B*). Neither of these two strains grew on minimal medium without pyridoxal (Fig. 5, *A* (*TMM*, *1* and *2*) and *B* (● and ○)), whereas addition of pyridoxal rescued the growth of both strains (Fig. 5, *A* (*TMM+pyridoxal*, *1* and *2*) and *B* (▼ and △)). When the expression of Pdx1 was induced by addition of 2% xylose, no growth was observed in the absence of added pyridoxal (Fig. 5*A*, *−YaaE* and *TMM+xylose*, *2*). However, when IPTG was included in the medium, growth was observed, implying that under these conditions prototrophy is absolutely dependent on YaaE (Fig. 5, *A* (compare *−YaaE(−IPTG)* and *+YaaE(+IPTG)* of *TMM+xylose*, *2*) and *B*, ■). This indicated complex formation between Pdx1 and YaaE in *B. subtilis*. Moreover, the growth rate approaches the values observed when the medium is supplemented with pyridoxal. The control strain did not grow under these conditions (Fig. 5, *A* (*+YaaE(+IPTG)* and *TMM+xylose*, *1*) and *B*, □).

In agreement with the *in vivo* complementation results, YaaE partially activated Pdx1 as monitored by its ability to synthesize PLP (Fig. 5*C*). However, even with a 1:5 molar ratio of Pdx1 to YaaE, PLP synthesis is only 50% of that observed with a 1:1 molar ratio of Pdx1 and -2 (Fig. 5*C*). These results clearly show that maximum PLP synthase activity depends on species-specific interactions of the two subunits, because an isofunctional subunit of another species is not able to fully re-constitute PLP synthase activity of the species-specific complex.

DISCUSSION

P. falciparum possesses a functional vitamin B6 biosynthesis pathway (5, 6). The plasmodial PLP synthase is a typical class I GATase consisting of the glutaminase subunit, Pdx2, that produces ammonia from glutamine and the synthase subunit, Pdx1, which most likely tunnels the reactive intermediate to the second active site where PLP is formed from ammonia, a pentose, and a triose. *Pdx1* and *Pdx2* are expressed throughout the erythrocytic cycle of *P. falciparum*, and both were shown to be cytosolic proteins thus able to functionally interact and generate vitamin B6 in these developmental stages of the parasites. In addition to the absence of this metabolic pathway from the human host, these are prerequisites that possibly make vitamin B6 biosynthesis a novel antimalarial drug target. This hypothesis is supported by reports that of the water-soluble vitamins present in blood plasma and culture medium only pantothenic acid or vitamin B5 appear to be absolutely required for parasite growth (47). However, it cannot be excluded that vitamin B6 is taken up by the parasite especially when considering reports about pyridoxine and PLP uptake by human erythrocytes and their interaction with hemoglobin (48, 49). Whether specific uptake mechanisms exist in the parasitized erythrocyte needs to be addressed in future studies, although genome analyses do not suggest the presence of a transporter

specific for pyridoxal or its derivatives similar to those found in *S. cerevisiae* and in *Schizosaccharomyces pombe* (50, 51).

The functionality of Pdx1 and Pdx2 in PLP biosynthesis was analyzed using the recombinant proteins. Both ribose 5-phosphate and ribulose 5-phosphate, as well as G3P and DHAP, are substrates for the plasmodial PLP synthase (Fig. 2, *C* and *D*), implying that it possesses a ribose-5-phosphate isomerase and triose phosphate isomerase activity as does YaaD (18, 19). With 92.1 pmol min^{-1} mg^{-1}, the specific activity of the plasmodial PLP synthase approaches that of the *B. subtilis* PLP complex (140 pmol min^{-1} mg^{-1}). Similar to YaaD, Pdx1 alone has no detectable PLP synthase activity with any of its substrates when glutamine is used as the ammonia donor (19). This is overcome when glutamine is substituted by ammonium sulfate. In that case, activity of Pdx1 depends on G3P as C3 sugar, whereas DHAP cannot be used as triose substrate in the absence of Pdx2, implying a lack of triose isomerase activity unless the bi-enzyme complex is formed. This is remarkable, because isomerization is thought to occur in the active site of Pdx1, which in analogy to other class I GATases is supposed to be on the opposite side of the Pdx1-2 interface. Similar to Pdx1, YaaD exhibits PLP synthase activity in the absence of YaaE, if ammonium sulfate is used as an ammonia donor. However, in contrast to the plasmodial system, it is the isomerase activity for the pentose sugar that seems to be dependent on complex formation, because only ribose 5-phosphate can be used as the C5 sugar under these conditions (19). These results emphasize the differences occurring between the PLP synthase complexes of these two organisms.

The overall layout of class I GATases requires a stoichiometric bi-enzyme complex. For the plasmodial Pdx1-2 complex, this functional model is supported by kinetic analyses that identified a 1:1 molar ratio as optimal for glutaminase activity (Fig. 2*A*). These results confirm those of Wrenger *et al.* (6). The presence of a complex between Pdx1 and Pdx2 *in vivo* was further corroborated by our findings that co-expression of Pdx1 and -2 resulted in a near stoichiometric complex formation of the purified recombinant proteins (Fig. 3*A*, *lane 4*). The necessity for the formation of a protein-protein complex was also supported by the results that Pdx1 rescues the growth of a YaaD-deficient *B. subtilis* strain only when YaaE expression is also induced during the complementation assay (Fig. 5, *A* (+*YaaE*(+*IPTG)* of *TMM*+*xylose*, *2*) and *B*, ■). This is confirmed by the *in vitro* studies with the recombinant parasite and bacterial proteins albeit the cross-species interaction between Pdx1 and YaaE result in sub-optimal PLP biosynthesis (Fig. 5*C*). Thus, it can be concluded that the interaction between glutaminase and synthase subunit has species-specific features.

Three major findings in the three-dimensional structure indicate how activation of Pdx2 could take place: 1) Cys^{87} of the catalytic triad is observed in two side-chain conformations (Fig. 4, *B* and *C*). The orientation with lower occupancy superimposes that identified in the structure of HisH (1GPW) the glutaminase subunit of *Tm*ImGPS, whereas the second one with higher occupancy superimposes that identified in the structure of the HisH/F complex (1K9V (39)) and with structures where either substrate or inhibitor are covalently bound (38). Thus, Cys^{87} in Pdx2 must attain this conformation during catalysis. 2) Oxyanion hole formation is a general principle among enzymes with catalytic triads stabilizing the transient negative charge during the hydrolytic reaction. Within the triad GATase family, the oxyanion hole has been conclusively described for ImGPS (43, 52). In general, the oxyanion hole is formed by two amide nitrogens, one from the residues following the catalytic nucleophile and the second from an adjacent β-strand, referred to as the "oxyanion strand." In Pdx2, these amide nitrogens are part of the peptide bonds between Cys^{87}-Ala^{88} and Gly^{51}-Gly^{52}. The carbonyl oxygen of the latter peptide bond points toward the putative oxyanion hole and obstructs it (Fig. 4*C*). Activation of Pdx2 would thus require peptide bond isomerization, probably induced by the binding of Pdx1. If this mechanism is characteristic of this class of enzymes, the structure of Pdx2 shown here represents the resting state of the enzyme. 3) The activation of the glutaminase domain by the synthase could further be explained, if residues of the synthase subunit contribute to the glutaminase active site. Indeed, in the structure of His7, the bifunctional *S. cerevisiae* ImGPS, as well as in the crystallographic complex of HisH/HisF (1JVN) a glutamine in the loop connecting α4″ and β5 in the synthase subunit contributes a hydrogen bond from Gln^{379} carboxyamine nitrogen to the substrate (38, 39). In CPS (1KEE (36)), $Gln^{273}N\epsilon2$ makes a similar interaction. Because Pdx2 alone has no detectable residual glutaminase activity, the interaction with the synthase subunit could be crucial to stabilize a conformation required for glutamine binding and/or hydrolysis. Amino acids in Pdx2 that potentially interact with Pdx1 in the bi-enzyme complex were deduced from the His7 structure and the HisH/F complex. Besides β7 and β8, the interface also includes the loop region between β12 and α6 carrying the catalytic histidine and glutamate. The interaction in this region might stabilize a distinct conformation allowing the glutaminase to gain activity.

The structural similarity between Pdx2 and other class I glutaminases possibly excludes this protein as a suitable drug target. However, the specific interaction with the PLP synthase subunit Pdx1 and the substrate specificities of the latter strongly suggest that specific inhibition of the PLP biosynthesis pathway in the parasites is feasible. Structural analyses of the Pdx1-Pdx2 complex are underway to substantiate our present findings and to elucidate specific features that may be exploitable for the design of specific inhibitors. In addition the pathway is currently investigated by reverse genetics to test our hypothesis that it is essential for parasite survival.

REFERENCES

1. Kirk, K. (2001) *Physiol. Rev.* **81,** 495–537
2. Fitzpatrick, T., Ricken, S., Lanzer, M., Amrhein, N., Macheroux, P., and Kappes, B. (2001) *Mol. Microbiol.* **40,** 65–75
3. McConkey, G. A., Pinney, J. W., Westhead, D. R., Plueckhahn, K., Fitzpatrick, T. B., Macheroux, P., and Kappes, B. (2004) *Trends Parasitol.* **20,** 60–65
4. Roberts, F., Roberts, C. W., Johnson, J. J., Kyle, D. E., Krell, T., Coggins, J. R., Coombs, G. H., Milhous, W. K., Tzipori, S., Ferguson, D. J., Chakrabarti, D., and McLeod, R. (1998) *Nature* **393,** 801–805
5. Cassera, M. B., Gozzo, F. C., D'Alexandri, F. L., Merino, E. F., del Portillo, H. A., Peres, V. J., Almeida, I. C., Eberlin, M. N., Wunderlich, G., Wiesner, J., Jomaa, H., Kimura, E. A., and Katzin, A. M. (2004) *J. Biol. Chem.* **279,** 51749–51759
6. Wrenger, C., Eschbach, M. L., Muller, I. B., Warnecke, D., and Walter, R. D. (2005) *J. Biol. Chem.* **280,** 5242–5248
7. Wrenger, C., and Muller, S. (2004) *Mol. Microbiol.* **53,** 103–113
8. Bean, L. E., Dvorachek, W. H., Jr., Braun, E. L., Errett, A., Saenz, G. S., Giles, M. D., Werner-Washburne, M., Nelson, M. A., and Natvig, D. O. (2001) *Genetics* **157,** 1067–1075
9. Ehrenshaft, M., Bilski, P., Li, M. Y., Chignell, C. F., and Daub, M. E. (1999) *Proc. Natl. Acad. Sci. U. S. A.* **96,** 9374–9378
10. Ehrenshaft, M., and Daub, M. E. (2001) *J. Bacteriol.* **183,** 3383–3390
11. Mittenhuber, G. (2001) *J. Mol. Microbiol. Biotechnol.* **3,** 1–20
12. Osmani, A. H., May, G. S., and Osmani, S. A. (1999) *J. Biol. Chem.* **274,** 23565–23569
13. Padilla, P. A., Fuge, E. K., Crawford, M. E., Errett, A., and Werner-Washburne, M. (1998) *J. Bacteriol.* **180,** 5718–5726
14. Zalkin, H., and Smith, J. L. (1998) *Adv. Enzymol. Relat. Areas Mol. Biol.* **72,** 87–144
15. Raushel, F. M., Thoden, J. B., Reinhart, G. D., and Holden, H. M. (1998) *Curr. Opin. Chem. Biol.* **2,** 624–632
16. Belitsky, B. R. (2004) *J. Bacteriol.* **186,** 1191–1196
17. Dong, Y. X., Sueda, S., Nikawa, J., and Kondo, H. (2004) *Eur. J. Biochem.* **271,** 745–752
18. Burns, K. E., Xiang, Y., Kinsland, C. L., McLafferty, F. W., and Begley, T. P. (2005) *J. Am. Chem. Soc.* **127,** 3682–3683
19. Raschle, T., Amrhein, N., and Fitzpatrick, T. B. (2005) *J. Biol. Chem.* **280,** 32291–32300
20. Graeser, R., Wernli, B., Franklin, R. M., and Kappes, B. (1996) *Mol. Biochem. Parasitol.* **82,** 37–49
21. Trager, W., and Jensen, J. B. (1976) *Science* **193,** 673–675

22. Suetterlin, B. W., Kappes, B., and Franklin, R. M. (1991) *Mol. Biochem. Parasitol.* **46,** 113–122
23. Chulay, J. D., Haynes, J. D., and Diggs, C. L. (1983) *Exp. Parasitol.* **55,** 138–146
24. The Plasmodium Genome Database Collaborative (2001) *Nucleic Acids Res.* **29,** 66–69
25. Bhavsar, A. P., Zhao, X., and Brown, E. D. (2001) *Appl. Environ. Microbiol.* **67,** 403–410
26. Sakai, A., Kita, M., Katsuragi, T., and Tani, Y. (2002) *J. Biosci. Bioeng.* **93,** 334–337
27. Sakai, A., Kita, M., Katsuragi, T., Ogasaswara, N., and Y, T. (2002) *J. Biosci. Bioeng.* **93,** 309–312
28. Kyhse-Andersen, J. (1984) *J. Biochem. Biophys. Methods* **10,** 203–209
29. Mohrle, J. J., Zhao, Y., Wernli, B., Franklin, R. M., and Kappes, B. (1997) *Biochem. J.* **328,** 677–687
30. Collaborative Computational Project Number 4 (1994) *Acta Crystallogr. Sect. D Biol. Crystallogr.* **50,** 760–763
31. Bauer, J. A., Bennett, E. M., Begley, T. P., and Ealick, S. E. (2004) *J. Biol. Chem.* **279,** 2704–2711
32. Perrakis, A., Morris, R., and Lamzin, V. S. (1999) *Nat. Struct. Biol.* **6,** 458–463
33. Murshudov, G. N., Vagin, A. A., and Dodson, E. J. (1997) *Acta Crystallogr. Sect. D Biol. Crystallogr.* **53,** 240–255
34. Jones, T. A., Zou, J. Y., Cowan, S. W., and Kjeldgaard (1991) *Acta Crystallogr. Sect. A* **47,** 110–119
35. Ross-MacDonald, P. B., Graeser, R., Kappes, B., Franklin, R., and Williamson, D. H. (1994) *Eur. J. Biochem.* **220,** 693–701
36. Miles, B. W., Thoden, J. B., Holden, H. M., and Raushel, F. M. (2002) *J. Biol. Chem.* **277,** 4368–4373
37. Tesmer, J. J., Klem, T. J., Deras, M. L., Davisson, V. J., and Smith, J. L. (1996) *Nat. Struct. Biol.* **3,** 74–86
38. Chaudhuri, B. N., Lange, S. C., Myers, R. S., Chittur, S. V., Davisson, V. J., and Smith, J. L. (2001) *Structure* (*Camb.*) **9,** 987–997
39. Douangamath, A., Walker, M., Beismann-Driemeyer, S., Vega-Fernandez, M. C., Sterner, R., and Wilmanns, M. (2002) *Structure* (*Camb.*) **10,** 185–193
40. Thoden, J. B., Holden, H. M., Wesenberg, G., Raushel, F. M., and Rayment, I. (1997) *Biochemistry* **36,** 6305–6316
41. Ollis, D. L., Cheah, E., Cygler, M., Dijkstra, B., Frolow, F., Franken, S. M., Harel, M., Remington, S. J., Silman, I., and Schrag, J., *et al.* (1992) *Protein Eng.* **5,** 197–211
42. Thoden, J. B., Miran, S. G., Phillips, J. C., Howard, A. J., Raushel, F. M., and Holden, H. M. (1998) *Biochemistry* **37,** 8825–8831
43. Korolev, S., Skarina, T., Evdokimova, E., Beasley, S., Edwards, A., Joachimiak, A., and Savchenko, A. (2002) *Proteins* **49,** 420–422
44. Chittur, S. V., Chen, Y., and Davisson, V. J. (2000) *Protein Expr. Purif.* **18,** 366–377
45. Zhu, J., Burgner, J. W., Harms, E., Belitsky, B. R., and Smith, J. L. (2005) *J. Biol. Chem.* **280,** 27914–27923
46. Ogasawara, N. (2000) *Res. Microbiol.* **151,** 129–134
47. Divo, A. A., Geary, T. G., Davis, N. L., and Jensen, J. B. (1985) *J. Protozool.* **32,** 59–64
48. Benesch, R. E., Yung, S., Suzuki, T., Bauer, C., and Benesch, R. (1973) *Proc. Natl. Acad. Sci. U. S. A.* **70,** 2595–2599
49. Ink, S. L., and Henderson, L. M. (1984) *Annu. Rev. Nutr.* **4,** 455–470
50. Stolz, J., and Vielreicher, M. (2003) *J. Biol. Chem.* **278,** 18990–18996
51. Stolz, J., Wohrmann, H. J., and Vogl, C. (2005) *Eukaryot. Cell* **4,** 319–326
52. Chaudhuri, B. N., Lange, S. C., Myers, R. S., Davisson, V. J., and Smith, J. L. (2003) *Biochemistry* **42,** 7003–7012
53. DeLano, W. L. (2002) *The PyMOL Molecular Graphics System*, DeLano Scientific, San Carlos, CA

SUPPLEMENTAL DATA

Supplementary Fig. 1. A C-terminal hexa-histidine tag was added to the protein sequence of Pdx2 to facilitate protein purification. This tag is involved in crystal contacts between two symmetry related chains. Side chains of all residues, His222 through His227, are visible in the electron density (not shown). Two tag sequences run antiparallel and a number of hydrogen bonding contacts between the heterocyclic nitrogen atoms of the histidine side chain and main chain carbonyl oxygen`s stabilise this arrangement. The pH of the crystallisation buffer was 6.0 at which the histidine side-chain is expected to be doubly protonated. The C-terminal carboxylate likewise is involved in two hydrogen bonds. This interaction is thought to have improved crystal quality as it provides a stable protein-protein contact in the crystal.

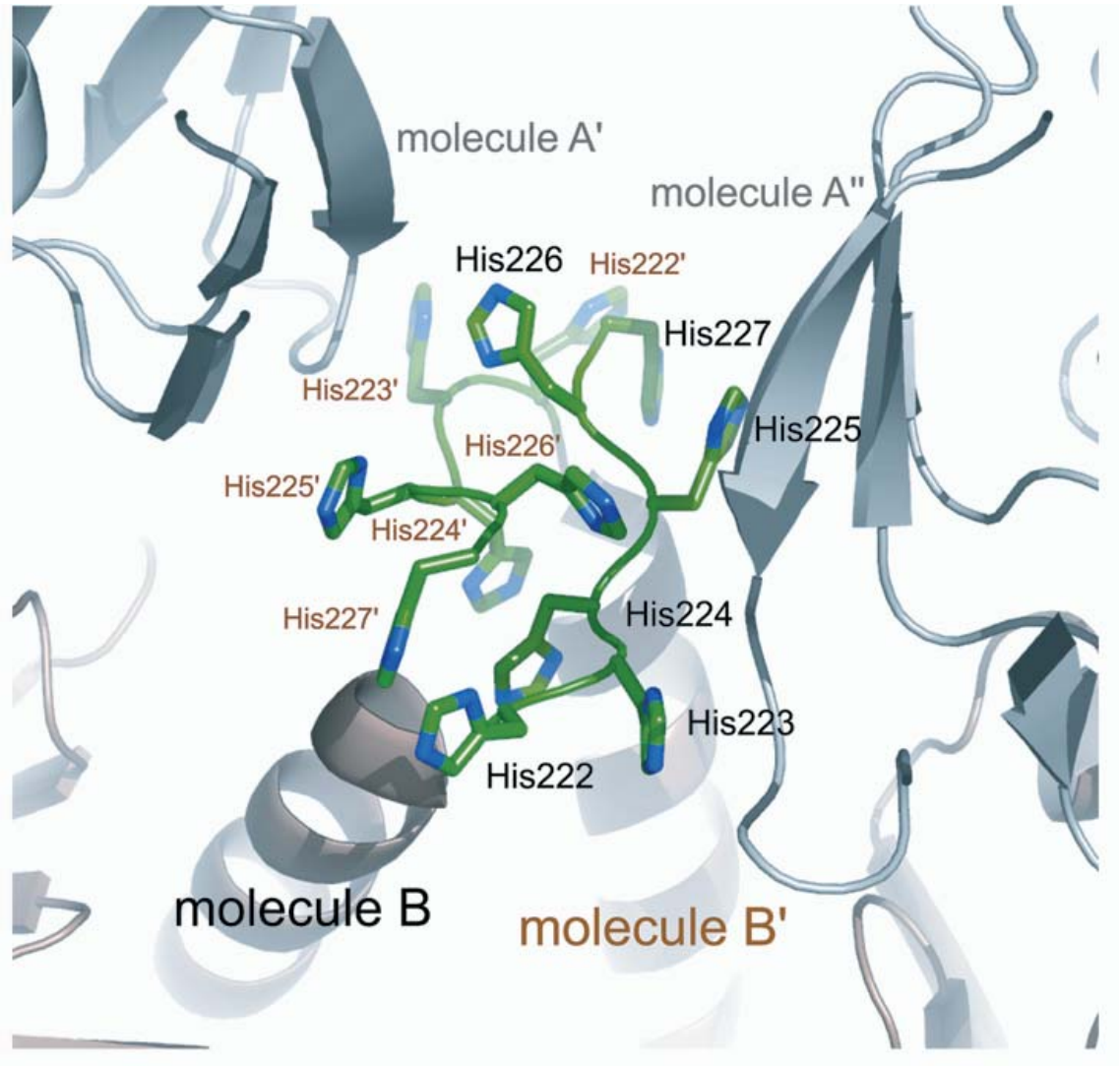

Supplementary Fig. 2**.** *Structure based sequence alignment of Pdx2, PbPdx2, HisH and YaaE*. Secondary structure elements are shown for *Pdx*2 and YaaE. The catalytic triad is marked with black triangles below these sequences. The green circles mark those residues that participate in the interface of the HisH/HisF bi-enzyme complex. The figure was prepared with ALSCRIPT (54).

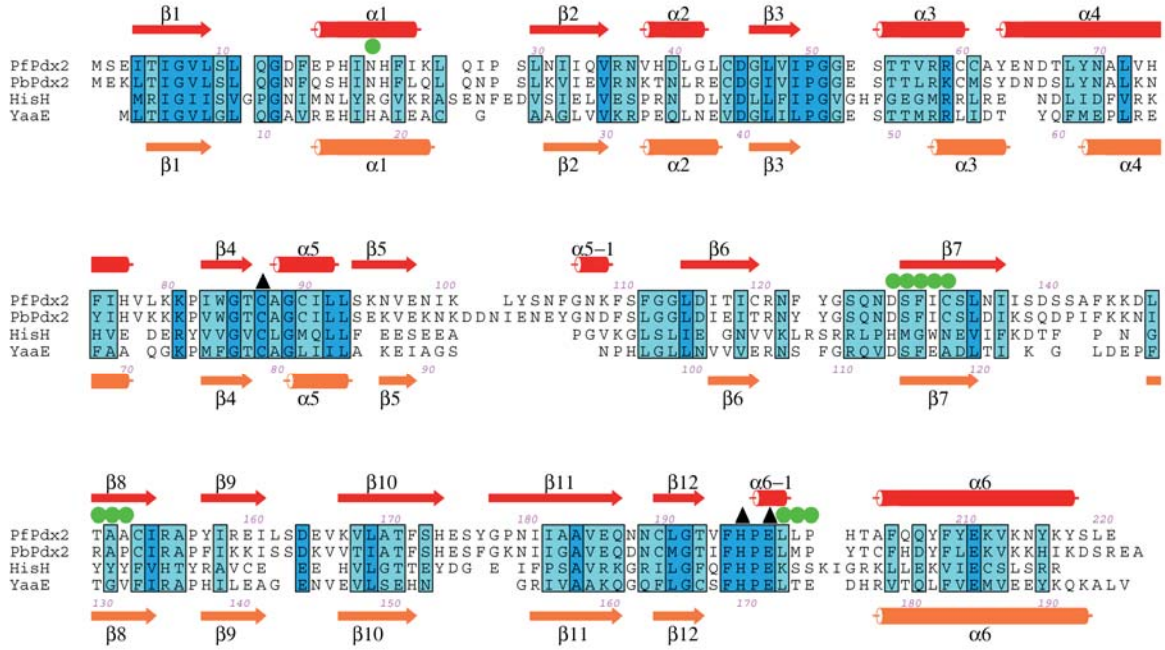

Supplementary Fig. 3**.** *Cellular fractions of* P. falciparum *infected red blood cells* - Coomassie Brilliant Blue stained SDS-PAGE gel (12%); uRBC – unifected red blood cell (control), iRBC – infected red blood cell, Para – parasite; M - membrane and C- cytosol are specifying the respective cellular fraction. Fifteen μg of each fraction was loaded.